The Effect of Probe Pressure on In Vivo Single Fiber Reflectance Spectroscopy

Ali Akbar Shakibaei

Submitted to the
Institute of Graduate Studies and Research
in partial fulfillment of the requirements for the Degree of

Master of Science
in
Physics

Eastern Mediterranean University
January 2014
Gazimağusa, North Cyprus

Approval of the Institute of Graduate Studies and Research

Prof. Dr. Elvan Yılmaz
Director

I certify that this thesis satisfies the requirements as a thesis for the degree of Master of Science in Physics.

Prof. Dr. Mustafa Halilsoy
Chair, Department of Physics

We certify that we have read this thesis and that in our opinion it is fully adequate in scope and quality as a thesis for the degree of Master of Science in Physics.

Assist. Prof. Dr. Sanaz Hariri Tabrizi
Co-Supervisor

Prof. Dr. Ozay Gurtug
Supervisor

Examining Committee

1. Prof. Dr. Mustafa Halilsoy

2. Prof. Dr. Ozay Gurtug

3. Assoc. Prof. Dr. S. Habib Mazharimousavi

ABSTARCT

Reflectance spectroscopy is a method to noninvasively quantitate the scattering and absorption properties of a turbid medium like tissue. The absorption and scattering properties can be used in diagnosis of different diseases such as cancer. Dependence of the acquired spectra to the environmental and physiological factors like probe pressure and habits of the person are being sought out in this thesis.

Our applied method, single fiber reflectance (SFR) spectroscopy, uses a single fiber for delivery and detection of the visible light. The SFR spectrum can be fitted by a nonlinear model of the scattering and absorption properties of the tissue under investigation.

In this study, SFR measurements are made by a fiber-optic probe gently placed on the lip tissue of some volunteers. The effect of variation in the probe pressure during the measurements is evaluated through the probable change in the extracted parameters from the fitted spectra. In order to do this, first the most appropriate model for the human lip reflectance spectrum is found. Then, the variation in the extracted parameters due to different probe pressures or physiologic characteristics of the volunteers is investigated.

Keywords: reflectance spectroscopy - single fiber reflectance spectroscopy

ÖZ

Yansıtma Spektroskopisi, doku gibi bulanık bir ortamın saçılma ve soğurma özelliklerini non invaziv bir şekilde niceleştiren bir yöntemdir. Soğurma ve saçılma özellikleri, kanser gibi çeşitli hastalıkların teşhisinde kullanılabilir. Bu tezde, elde edilen spektrumun prob baskısı ve kişinin alışkanlıkları gibi çevresel ve fizyolojik faktörlere bağlı olup olmadığı aranmaktadır.

Uyguladığımız yöntem olan Tek Fiber Yansıma (SFR) Spektroskopisi, görünür ışık iletimi ve saptanması için tek bir fiber kullanmaktadır. SFR spektrumu, araştırmakta olduğumuz dokunun saçılma ve soğurma özelliklerinin doğrusal olmayan bir modeli ile incelenebilir.

Bu çalışmadaki SFR ölçümler, bazı gönüllülerin dudak dokularının üzerine yavaşça yerleştirilen bir fiber -optik prob ile yapılmıştır. Ölçümler boyunca gerçekleşen prob basıncındaki değişimlerin etkisi, grafiklerden elde edilen parametrelerin olası değişimleri dikkate alınarak değerlendirilmiştir. Bunu yapabilmek için öncelikle insan dudak yansıtma spektrumuna en uygun model bulunur. Son olarak, parameterler üzerinde, farklı prob baskılarına bağlı olarak veya gönüllülerin fizyolojik özellikleri nedeniyle ortaya çıkan variyasyonlar incelenmiştir.

AnahtarKelimeler: yansıma spektroskopisi, tek fiber yansıma spektroskopisi

To whom it must be concerned and

those who I adore

ACKNOWLEDGEMENTS

My indebt to my family members, who have ever done their best for me, makes me to present my gratitude to them. My special thanks and deepest heart felt appreciation goes to Ms. Dr. Sanaz Hariri Tabrizi for her immense knowledge, continuous support, patience, honest companionship and her gracious heart. It is not exaggerated if I say that she emerged in my life as a miracle. She actually revived me, my motivation and effort, and reminded me the sense of humanity. I could not have imagined having a better co-supervisor for my master studies. I would also like to thank Prof. Mustafa Halilsoy, Prof. Ozay Gurtug, my dear supervisor, and Prof. Habib Mazharimousavi for their assistance within this educational period. Moreover, I would like to thank Ms. Cilem Aydintan, dutiful and kind secretary, who helped me so much. Last but not the least, my thanks to Jalil Heydaripour, Ehsan Bahramzadeh, who while he was busy, he helped me out to remove my thesis-related problems, Morteza Kerachian, Mehrdad Khamooshi, Ali Hooshyar and Iman Roozbeh who had fun together.

TABLE OF CONTENTS

LIST OF TABLES

LIST OF FIGURES

LIST OF SYMBOLS

Chapter 1

INTRODUCTION

1.1 Optical Properties of Tissue

Due to effective and important role of light for different applications in the biological tissues during the recent decades, investigating new methods to measure optical properties has been developed [1]. Variations in the optical properties of tissue indicate noticeable structural changes like those happen in the (pre)cancerous conversion of epithelial tissue. For instance, alterations in the absorption coefficient can be attributed to blood oxygenation and tissue metabolism [2]. On the one hand, light is able to go through a tissue, interact with tissue components and finally leave the tissue, and this ability is known as a key to diagnostic applications of light. On the other hand, light is able to enter the medium and release energy through the tissue absorption characteristics. This ability is basic to therapeutic use of light. Therefore, first step is to recognize the optical characteristics of tissue to appropriately design and translate diagnostic measurements, and to predict the light distribution and energy release, the second stage is to apply the properties in a model describing light transport. As a very important example for the second step, Monte Carlo methods can be referred as one of the main models for photon propagation in the biological tissues. This model is based on probabilistic models and studies photon trajectory inside the tissue [1].

1.2 Light Propagation in the Tissue

In a turbid medium, in which light scattering by its nonuniformities has noticeable intensity, photons propagate in all directions by scattering or absorption. The properties of photon propagation including scattering and absorption events within the tissue, reflection and transmission control the number of photons that will reach to point r. As shown in Fig.1, the changes in photon direction during propagation suggest that definitely a huge number of scattering events take place for photons individually. Between 400 and 1200 nm, near IR and visible wavelengths, scattering is a significant event in tissue, and the mean length traversed by a photon between two scattering points is around 0.01–0.2 mm. In addition to scattering, photons can be absorbed by chromophores, tissue components that absorb light; they are able to be internally reflected at the interface; and/or also they can finally leave the tissue [2].

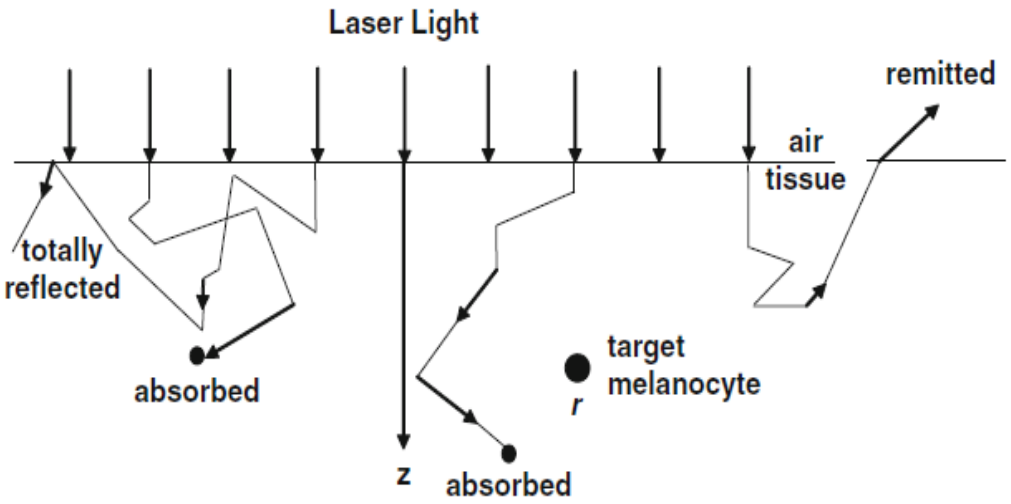

Figure 1. Random paths of photons propagation

1.2.1 Scattering

During light propagation through the tissue, optical scattering is considered as an event caused by either particles with a refractive index which is different from the refractive index of the surrounding medium. Mie theory is a solution considered by Gustav Mie to the light scattering problem by spherical particles of any size. In this theory, ‘particles’ are known as an aggregation of material containing an area with refractive index which is different from the refractive index of the surrounding medium. The calculation results show that scattering coefficient is associated with multiplication of number density of scatterer by the scattering corss-sectional area. Rayleigh and Mie scatterings are commonly the main scattering interaction in the IR – visible wavelength range. Although Rayleigh scattering is applied for particles that are small with respect to wavelengths of light, it should be taken into consideration that actually Mie scattering is a well-known name for scattering according to spheres of all sizes. The word Rayleigh scattering originated from the Rayleigh limit of Mie scattering [3].

If we use a laser source, as monochromatic and coherent source, we can see the dependence of the scattering intensity to time which is attributed to Brownian motion that makes the scatterers in the solution to change constantly with time. The scattered light affects the surrounding particles. In this fluctuation limit, information contains the time criteria of movement of scattering bases. Autocorrelation function helps us to derive information of the particles from an experimentally recorded intensity trace autocorrelation. Tissue scattering is described by continuum scattering theory as autocorrelation function that explains spatial distribution of the refractive index in a turbid medium [1].

1.2.2 Absorption

Absorption accounts for light attenuation in the tissue. During this phenomenon, photon transmits its energy to the molecules and leads to molecular or electronic vibrational states. The interaction is dependent on the wavelength of the incident light. Also, it depends on the tissue type and chromophores. Beer-Lambert law shows that absorption coefficient μ_a describes how far a photon can penetrate into the tissue before being absorbed. Because of high absorption of Hb and water in respectively UV and IR wavelength regions, this region is known as therapeutic region. Typical values of μ_a are from 0.5 (cm^{-1}) to 5 (cm^{-1}) in the VIS and IR regions.

According to what briefly described as the basic events during light propagation inside turbid medium, optical properties of tissues include absorption coefficient μ_a (cm^{-1}), scattering coefficient μ_s (cm^{-1}), the probability density function and refractive index of the tissue is n [1,2].

To express the absorption and scattering coefficients, as the main tissue optical characteristics, consider a photon which is propagating over ds. They can be defined as:

- The absorption probability of a photon in interval ds is $\mu_a ds$.
- The scattering probability of a photon in interval ds is $\mu_s ds$.

The probability density function for scattering is defined as the probability that scattering occurs from a certain direction into another direction (sometimes called the phase function of single particle scattering). Because of few or a single scattering events, when thin tissue sections are studied, $p(\theta,\psi)$ is proper, but in thicker tissues since there are multiple scattering events and directions of scattering forms in the

tissue are directed by accident, consequently the dependence of scattering on ψ is meant and neglected, and the multiple scattering averages the θ so that we have g = <cosθ> , that we call it as anisotropy factor. In addition to anisotropy factor, reduced scattering coefficient $\mu_s' = \mu_s(1-g)$ is another factor that plays a main role in describing scattering properties [4].

1.3 In Vivo Methods

1.3.1 Some Approaches Based on In Vivo Methods

Non-invasive use of these methods has made these methods more useful for practical medical applications than ex vivo methods. There are different ways to categorize the methods that has so far been used customarily, but here we preferably introduce the methods according to a classification based on the illumination source, steady state and time dependent methods. Some in vivo spectroscopy methods to evaluate the human tissue are as following:

Steady state: For determination of tissue optical properties we can use following approaches:

- Spatially resolved:

In spatially resolved spectroscopy reflectance measurements at different distances from the incident light beam are combined to obtain sufficient information for the separation of the scattering and absorbance properties. Since the diffuse reflectance is measured at several distances, a distinction can be made between light that traveled shorter distances through the tissue (low penetration, less interaction with the tissue) and light that propagated through the tissue for longer times and distances (penetrated deeper and more interaction). Moreover in the case of multilayered tissue, the light captured at shorter distances contains almost only information on the top layer while at longer distances the collected light is influenced by the top layer as

well as underlying layers. These multiple measurements at different distances are then combined with light propagation models to determine the absorption and scattering properties of the different disuse layers. The acquired optical properties can then be related to the composition and microstructure of the product Fig.2.

- Spectrally constrained:

In Spectrally constrained measurement R(r) is second type of steady state measurement, and as shown in Fig.3, in this method reflectance is evaluated with respect to wavelength. Major application of these methods is studying the chromophores of tissue including water and oxyhemoglobin and deoxyhemoglobin.

Time dependent: These methods are suitable for deeper examination (> 1 cm) in the tissue. For determining the optical properties of tissue we can use the following approaches:

- Time resolved: It uses picosecond pulses and measures the tissue response:

Time resolved reflectance methods are based on measurement of the response of the tissue. The input signal is picosecond pulse and the reflectance is measured depending on time in a distance around source. These methods are advantageous due to possibility of optical properties determination from direct metrics as time-to-maximum and final logarithmic slope. Fig.4 shows the principle of measurement.

- Frequency domain: It depends on determination of the phase shift and amplitude modulation, incident beam is frequency modulated:

In this mode the source intensity is modulated at different frequencies. It is analogical to the Fourier transform of time resolved measurement and carries no additional information. But still has its advantages in acquisition time and data analysis.

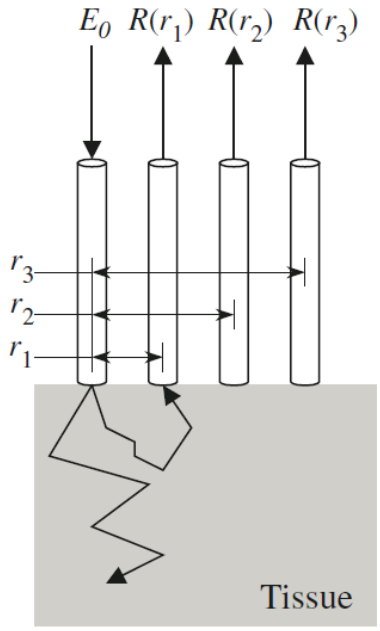

Figure 2. Spatially resolved diffuse reflectance

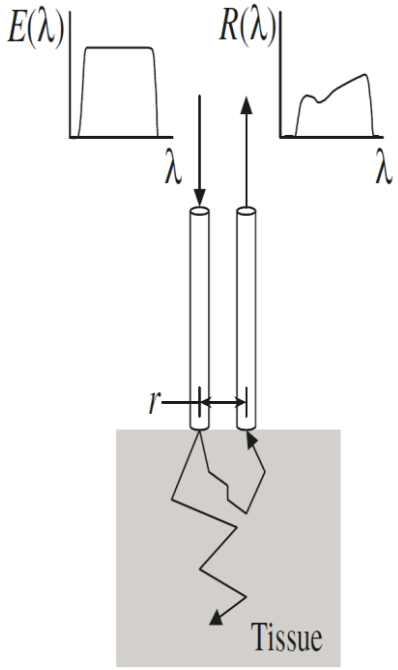

Figure 3. Measurement method of spectrally constrained diffuse reflectance

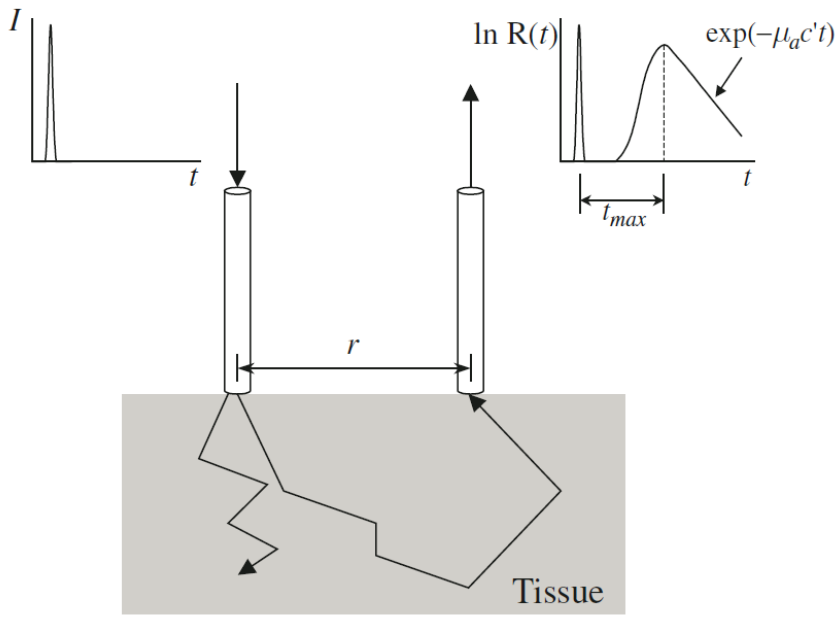

Figure 4. Measurement of time-resolved diffuse reflectance

The methods briefly introduced above are quite complex and involve relatively expensive equipment. Also such classical reflectance spectroscopy devices often use multiple optical fibers for delivery and collection of light. Moreover, to satisfy the validity of the theoretical aspect, some of them need great source-detector separations. Accordingly, the traced photons passed a long path through the tissue and the ultimate results give mean values over a big volume of tissue. Unlike the mentioned situation, a major necessity to detect the precancerous lesions is detecting the subtle changes inside or just below the mucosa in a small volume. Hence, a diagnostic tool to investigate the optical features of the top layer of the tissue is required [5].

1.3.2 Single Fiber Spectroscopy

In this study, we applied single fiber reflectance spectroscopy (SFR) with the system setup shown in Fig.5. It contains a single optical fiber for delivering light to the sample and collecting the remitted light from the tissue. During the measurement, photons from the source go through one arm of a bifurcated fiber and the single fiber,

after which they penetrate into the sample. Photons reflected from the sample go through the second branch of the bifurcated fiber and finally to the spectrophotometer. Advantages including small size of the probe and simple design of the device make it more beneficial for some specific applications.

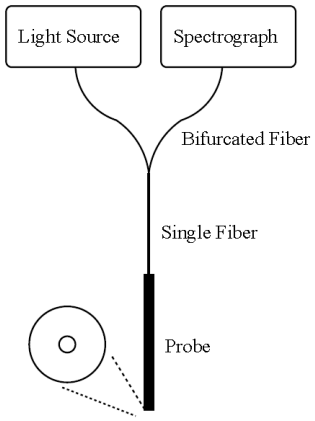

Figure 5. SFR system

Chapter 2

BACKGROUND AND LITERATURE SURVEY

In the past, single fiber configurations were applied to study fluorescence in tissue and phantoms and to analyze the size of particles. The effect of probe pressure in fluorescence [6-9] and reflectance [6, 8, 10, 11] spectroscopy has been discussed by several researchers. Nath et al. [9] investigated this influence on fluorescence spectra of the cervix. Menopausal status and age affect cervical measurements. Nath +et al. studied fluorescence excitation emission matrices in twenty volunteers at three different pressures. They analyzed the data obtained from spectroscopy and compared the fluorescence intensities with respect to pressure. They examined the intensity differences at each excitation/emission wavelengths pair. At three levels of pressure, abnormal tissue demonstrated lower fluorescence intensity than normal tissue, and patients with post-menopausal displayed greater fluorescence intensity than pre-menopausal patients. The analysis ultimately indicated that pressure did not mainly change the fluorescence intensity. In another study on the cervical tissue, Rivoire et al. [7] took repeated measurements to show if the measurement order causes change in the fluorescence spectra and if there are differences due to pressure variation. They compared the fluorescence intensity at three calibrated levels of pressure (0.2, 0.4, 0.6 N). The measurements were taken from eighteen patients, and after corrections for multiple comparisons, it was shown that neither the probe pressure order nor the compatibility of probe pressure were highly effective on variations in fluorescence intensity. Therefore, the probe pressure variability is

probably not an issue for these devices.

On the contrary, Reif et al. [10] found conflicting results from their study on mouse thigh muscle in terms of pressure. They studied in vivo reflectance measurements obtained from mouse muscle under various pressure of the probe. They anesthetized ten mice, removed each muscle skin and placed the probe perpendicular to tissue surface to take the measurements. Consequently it was found that the pressure values applied to the thigh muscle was effective on the reflectance spectrum. Also, after fitting the analytical model to the reflectance spectra, it was shown that vessel size and hemoglobin saturation decreased significantly while scattering increased.

Short- and long-term influences of various probe contact pressures on fluorescence and diffuse reflectance spectra were studied by Ti et al. [8] They obtained the fluorescence and diffuse reflectance spectra from the heart and liver of rat using a mechanical arm to place the probe on the tissues The results indicated that too much probe pressure disturbs the hydrodynamics of the examined tissue that causes the apparent spectral changes due to a reduction in blood oxygenation, blood volume and perhaps tissue metabolism. It was mentioned that these variations may strongly depend on the tissue and application of the spectroscopy techniques. Atencio et al. [11] investigated the influence of probe pressure on diffuse reflectance spectra of human skin. The study was performed on forty five patients. The patients were asked to rest their forearms to contact the probe under five pressure levels, and then the diffuse reflectance spectra were acquired. Atencio et al. [11] found a decrease in intensity of diffuse reflectance above 600 nm in 83% of cases while there was no significant difference in spectral band of 400-600 nm. Applying reflectance and fluorescence spectroscopy, Lim et al. [6] also conducted a relatively similar study on skin and consequently found that short-term (< 2 s) effects of probe pressure (P <

$9*10^{-3}$ N/mm^2) are less than 0 ± 5% for diagnostically significant physiologic properties of the tissue.

Since SFR measurement is made by a fiber probe gently placed on the sample, it is investigated if the probe could be a source of variation in the measurements. In the present study, the effect of varying probe pressure during the lower lip measurements in normal volunteers is evaluated.

Chapter 3

MATERIALS AND METHODS

3.1 SFR Model

3.1.1 Absorbers

Structure of lip was the main reason that we chose it for our study. The skin of lip, with three to five cellular layers, is very thin in comparison with typical face skin which consists of up to 16 layers. The skin of the lip contains fewer melanocytes when its color is light. Melanocytes produce melanin pigment and produce the color of skin. In darker skin color, since the skin of the lip has more melanin and thus it looks darker. Melanin has three types including eumelanin, pheomelanin and neuromelanin, while eumelanin is the most common type. Pheomelanin is a red-brown polymer that abundantly accounts for red hair and freckles. Neuromelanin is detected inside the brain, and its function is ambiguous. The process of producing melanin is called melanogenesis. Within the skin, this process occurs after the skin is exposed to UV radiation. Since melanin is an effective light absorber, it is thought that it protects the skin cell from UV radiation damage and reduces the risk of cancer. These characteristics of melanin encouraged us to consider it for further fitting process to know if we can choose it as the absorber(s).

Beta-carotene, a type of carotene, was chosen as the second material for fitting process. Carotene is an orange pigment that is found in blood and carotenaemia determines the availability of the carotene (orange pigment) in blood. Beta-carotene

is a strongly colored red-orange pigment that is effective on the color of skin. Although beta-carotene has been applied for various treatments of irregularities such as reduction of the risk of breast cancer in woman before menopause, it is debated if it is effective in treating different kind of cancer [12]. The use of beta-carotene in a recent study on cervical premalignancies [13] and similarity of the lip epithelium with cervix, made us to take this material into consideration for analysis.

In order to find the appropriate absorber(s) the SFR spectra were fitted by each absorber separately. As the first absorber, we used extinction coefficient spectrum of melanin that had been quantitatively obtained by Zonios et al. [14]. Figure 7 shows the extinction coefficient versus wavelength in the range between of 450-820 nm.

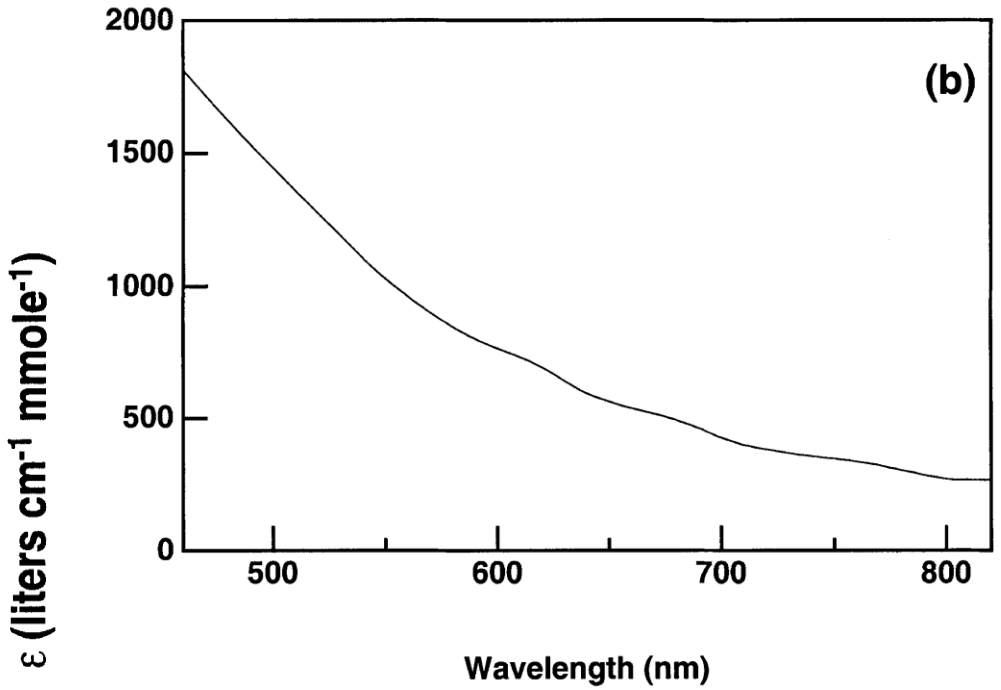

Figure 6. Molecular extinction spectrum of melanin

However, we needed this spectrum between 400-900 nm because the other required spectra such as Hb and HbO_2 were obtained for this range and that specially wavelength range between 400-600 nm is very important for blood characteristics.

Using the extinction coefficients of eumelanin and pheomelanin that were presented by Steven Jaques [16], Fig.8, and using Graph Digitizer Scout software for digitization and interpolation, we could find the spectrum in the required wavelength range. Then, we utilized the extinction spectra as the input data in the LabView program for the fitting process.

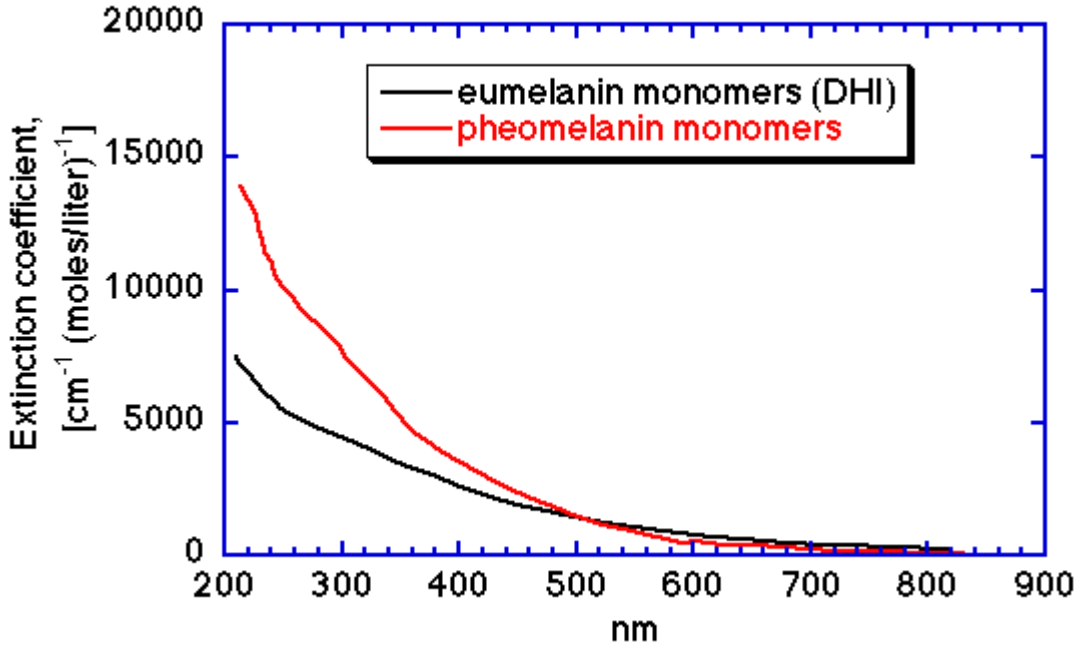

Figure 7. Extinction coefficient spectra of Eumelanin and Pheomelanin

For beta carotene, we had done the same as what we did for melanin. To check whether the absorbers were individually in good agreement with fitting requirements, from 288 spectra, 30 spectra were selected randomly. During fitting process that was performed by using LabView software, in order to find the best fitted spectrum related to each measurement number we had to adjust parameters include smoothing factor and pixel cut off. Smoothing factor averages the number of pixels according to what registered in the blank, Fig.8. In this study, the minimum amount for smoothing factor was 7 so that at least 7 pixels were averaged. Pixel cut off, which ranges from 205 to 215, removes the amount of the selected pixels and calculates the rest. Again,

in Fig.8, one can see that 207 was registered for pixel cut off that means 207 pixels are removed and the remained pixels are taken into consideration for fitting. In Figs. 8-11, four examples of acceptable and unacceptable fitted spectra associated with individual application of beta carotene and melanin are presented. There are three different spectra in each image colored as red, black and blue. The black one is the calibrated spectrum obtained from the volunteers, the red one presents the fitted spectrum and the blue one is the spectrum fitted by the initial guess coefficients. Obviously, the more consistent are red and black spectra, the more acceptable fitting we have. Mean square error (mse) and residual great are parameters that enable us to quantitatively find out whether a fitting is acceptable or unacceptable. Mse quantifies the difference between implied values and true values of the quantity being estimated (red and black spectra), Table 1. Therefore, we accepted spectra similar to those shown in Figs. 8 and 10 for statistical evaluation and rejected the rest. According to what mentioned about fitting process, since we could not get our favorite fitting from individual use of the absorbers, we decided to apply them together and investigate the result for this mode. Figures 12 and 13 are examples of the fitting process for the combined application of melanin and beta carotene.

To demonstrate the difference between individual and combined applications of absorbers in the fitting model of SFRS, Table 1 containing the goodness of fit parameters is presented.

Table1. Comparison of mean square error for three different absorbers

	Meas. No.	mse	Smoothin	Cut Off	Res Great
SingleMel	53	5.39634	7	207	25
	162	66.03716	9	205	65
SingleBCa	53	3.51575	7	207	13
	162	13.5646	8	207	47
Combined	53	3.40995	7	207	12
	162	10.086	8	215	37

One can see that the least mse and residual great is obtained when the absorbers are applied together in the SFRS fitting model. 99% of our data met this situation, and accordingly, we chose the combined mode for our further statistical operations.

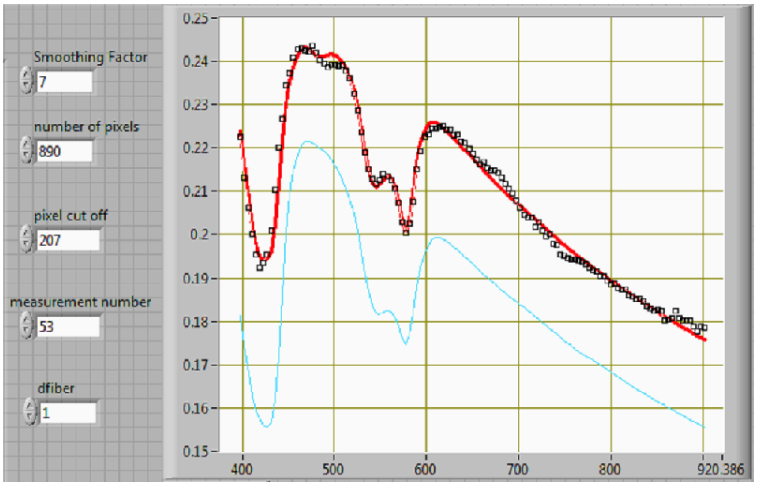

Figure 8. Beta Carotene

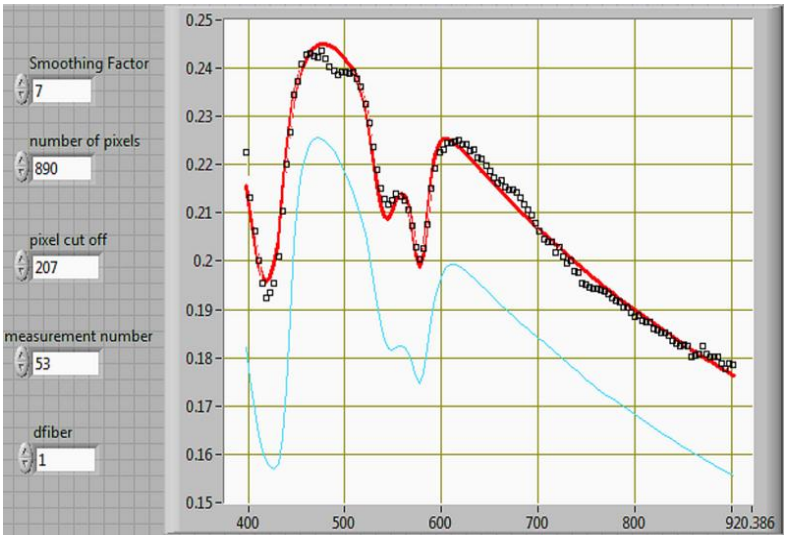

Figure 9. Melanin

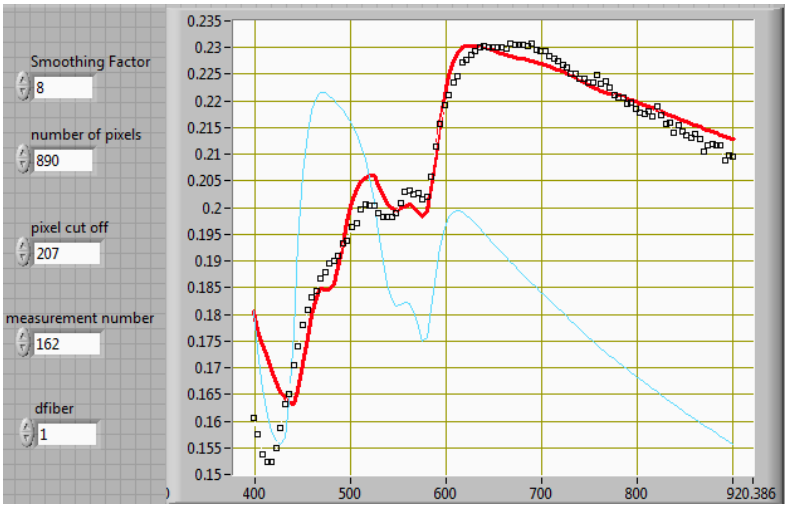

Figure 10. Beta Carotene

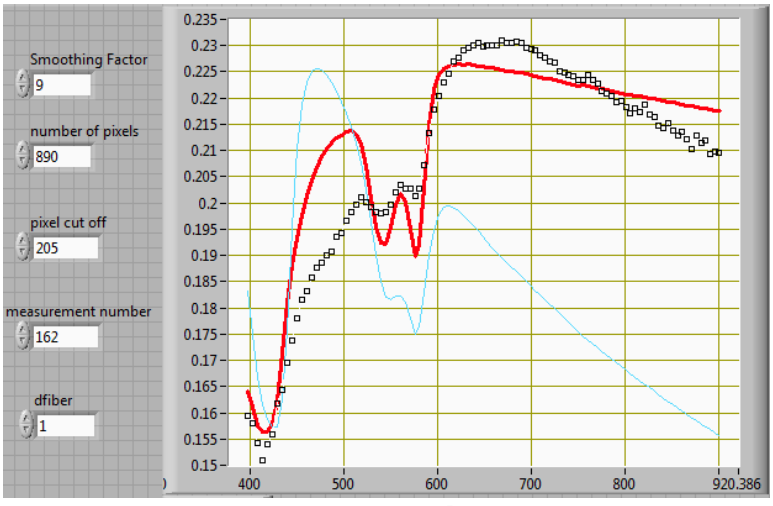

Figure 11. Melanin

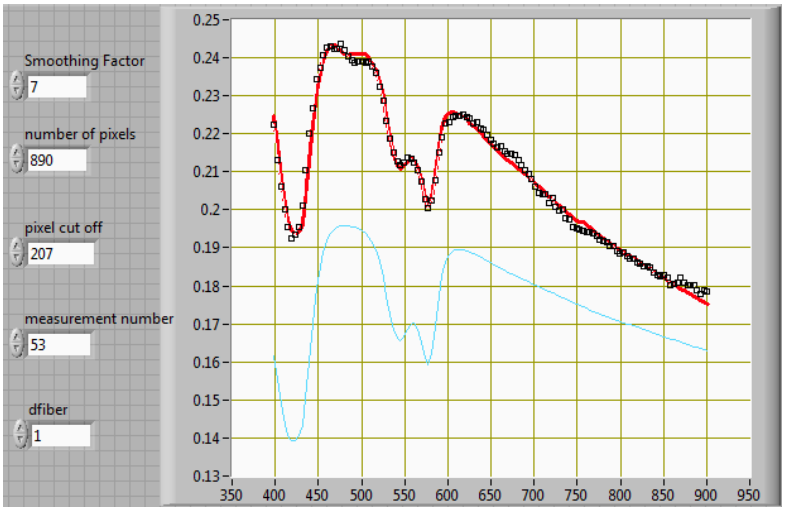

Figure 12. Beta Carotene & Melanin

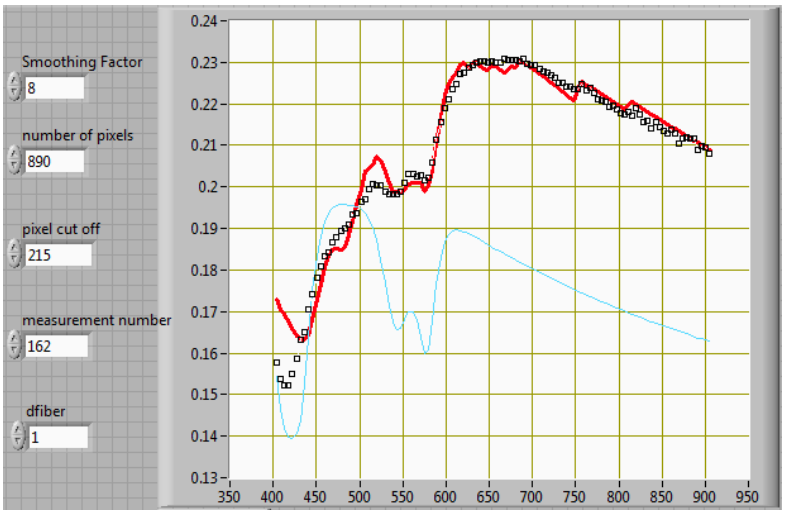

Figure 13. Beta Carotene & Melanin

Before finding the influence of different probe pressure, we removed the step-like points by converting them to a smooth curve. Figure 14 shows some step like pattern after 630 nm. It is due to the same pattern of the melanin spectra after digitization. The best solution was to smooth the extinction spectrum of melanin in the aforementioned wavelength range. Using the MATLAB sotware, we could fit the melanin spectrum by a 6th order polynomial with an R-squared value of 0.9921 Finally, the smoothed melanin extinction spectrum was used as an input for the SFR model, then all the spectra were fitted and classified using statistical data analysis.

3.2 Methods

3.2.1 Experimental Setup

Commercial constituents of the experimental setup for SFR measurements included an optical fiber spectrometer (AVASPEC-2048-USB2, Avantes Inc) and a tungsten halogen light source (AVALIGHT-HAL-S). A bifurcation was prepared using two 200 μm diameter optical fibers which connected the spectrometer and the light source to the contact probe. The common end of the fiber-optic probe was a 1000 μm diameter fiber with a numerical aperture of 0.22 that was surrounded by a stainless steel tube with a 1.6 mm outer diameter. In order to minimize specular reflection occurring at the tip of the probe tip due to the difference between refractive index of the sample and the fiber, the single probe tip was polished at an angle of 15° [16].

At the distal end of the probe a spring and a holder were designed in order to apply a specific pressure to the tissue during the measurement. Before the experiment, the linearity of the spring had been tested and it showed an R-square of 0.999 (data is not included).. A calibration process was done before the measurements in order to account for variability in lamp-specific output, in fiber-specific transmission properties and other internal reflections.

Here, the spectra were calibrated against a solid phantom consisting of Titanium dioxide (TiO_2) [4]. Figure 5 shows the experimental setup for the SFR system. Spectra were collected and saved using an interface written by LabView program (Version 7.1; National Instruments). These measurements were used to evaluate R^{SF} as:

$$\mathbf{R}^{\mathbf{SF}}=C\mathrm{cal}\left[\frac{(\boldsymbol{I}-\boldsymbol{I}\mathrm{water})}{(\boldsymbol{I}30-\boldsymbol{I}\mathrm{water})}\right] \quad (1)$$

3.2.2 Statistical Method

A semi-empirical model for SFR spectra analysis (1) has been described previously [13]. The constants in (1) were found based on Monte Carlo simulations of SFR measurements of a homogeneous turbid medium [17]. This model originates from the investigation about the relationship between SFR intensity and optical properties. A function was introduced that described the dependence of the effective path length of the photon on the optical characteristics of the sample. Since quantitative measurement of μ_s' improves the accuracy of the chromophores concentration estimations and provides information about the tissue microstructure, a methodology used to experimentally extract $\mu_s'$of the considered sample from SFR spectra by applying a mathematical model of $R^{SF}=f(\mu_s' d_{fiber})$ and a calibration phantom. Simulating the reflectance data, using Monte Carlo methods, and inspecting the data throughout the range of scattering features led to an objective relation between R^{SF} and $\mu_s' d_{fiber}$ as following:

$$R = \eta limit \times \left(1 + \rho 3 e^{-\rho 1 \mu_s' d_{fiber}}\right) \times \left[\frac{\left(\mu_s' d_{fiber}\right)^{\rho 2}}{\rho 1 + \left(\mu_s' d_{fiber}\right)^{\rho 2}}\right] \quad (2)$$

After the weighted residual error minimization, the parameters [ρ_1, ρ_2, ρ_3] were fitted, determined and finally caused Eq. (2) to change as Eq. (3):

$$R = 2.7 \times \left(1 + 1.55 e^{-6.82 \mu_s' d_{fiber}}\right) \times \left[\frac{\left(\mu_s' d_{fiber}\right)^{0.97}}{6.82 + \left(\mu_s' d_{fiber}\right)^{0.97}}\right] e^{-\mu_a L} \quad (3)$$

μ_s', μ_a and photon path length (L) are described in the subsequent equations (4-6) [17, 19]. The fiber diameter is indicated by d_{fiber} symbol and is in μm unit.

$$\mu_s' = a_0 \left(\frac{\lambda}{800}\right)^{a_1} + a_2 \left(\frac{\lambda}{800}\right)^{-4} \quad (4)$$

$$L = \frac{0.944 \times 1.54 \times d_{fiber}}{\left(\mu_s' d_{fiber}\right)^{0.18} \times \left(0.64 + \left(\mu_a d_{fiber}\right)^{0.64}\right)} \quad (5)$$

$$\mu_a = a_3 \rho \left[StO_2 \times \mu_a^{HbO_2} + (1 - StO_2) \times \mu_a^{Hb}\right] + a_6 \times \mu_a^{Bcar} + a_7 \times \mu_a^{melanin} \quad (6)$$

$$StO_2 = 0.5 + \left(\frac{\tan^{-1}(a_4)}{\pi}\right) \quad (7)$$

$$\rho = \frac{1-e^{-a_5\left[StO_2\times\mu_a^{HbO_2}+(1-StO_2)\times\mu_a^{Hb}\right]}}{a_5\times\left[StO_2\times\mu_a^{HbO_2}+(1-StO_2)\times\mu_a^{Hb}\right]} \quad (8)$$

where λ is the wavelength in nm, input spectra are extinction coefficients for fully oxygenated whole blood ($\mu_a^{HbO_2}$), fully deoxygenated whole blood (μ_a^{Hb}) [20], beta-carotene (μ_a^{Bcar}) [21] and melanin ($\mu_a^{Melanin}$) [14, 21]. The blood saturation (StO_2) is defined as (7) to impose an artificial boundary condition for this parameter to restrict it to [0,1] range [18]. The fitting parameters ($a_0 – a_7$) are Mie amplitude, Mie slope, Rayleigh amplitude, blood volume fraction, blood saturation, average vessel diameter, beta-carotene concentration and melanin concentration, respectively. We used a non-linear fitting algorithm, Levenberg-Marquardt, which was scripted into a LabView program (Version 7.1.1; National Instruments) to estimate the eight parameters.

Chapter 4

RESULTS AND DISCUSSION

We obtained a total of 288 spectra from the subjects. The spectra were obtained from thirty three normal volunteers (8 females, 25 males) who were randomly involved in this study with the age range of 21 to 38. Among the subjects, 5 men used to smoke cigarettes, three females and two males had blood deficiency. The measurements involved applying three levels of pressures to the right, middle and left lower lip. The levels of applied pressure were denoted as 1, 2 and 3. Measurements were acquired by the same user to eliminate inter-user variability. The highest pressure was chosen so as not to hurt the subject. A colorful indicator was used under the spring to visually guide the operator to apply the predetermined pressure. Five SFR spectra were averaged at each site. The spectra with a large deviation in the five spectra were discarded and the measurements were repeated. The effect of various probe pressures was determined by inspecting the change in the fitting parameters.

There are two kinds of statistics, named as parametric and non-parametric. In order to check the null hypothesis of equality of the mean or median values of two populations one of these methods should be applied. Parametric statistics necessitates satisfaction of three conditions including independence of the samples obtained from the populations, normal distribution of the populations and equal variance of the populations. In the cases that these assumptions are not satisfied or are debatable, non-parametric tests are applied.

Using non-parametric statistics, we investigated two circumstances including the effect of pressure changes on the reflectance spectra from each measured point and if smoking cigarettes affects the obtained spectra. For the first state, 8 parameters from three different applied pressures were classified into left, middle and right and considered independently. In the second state, we compared the eight parameters under three pressures in two smoking and non-smoking groups. In order to choose between the parametric or nonparametric tests, histograms of the eight parameters were drawn for each population. Most parameters did not distribute normally. , and consequently nonparametric tests were applied for the data analysis. Moreover, the result of the Levene test of equality of the variances confirmed this choice, Tables 2-7. It can be seen from the p values presented in Table 2 that vessel diameter and blood volume do not have the same variances. Table 3 shows the same phenomenon for melanin and beta-carotene and Mie slope and Table 4 for Rayleigh amplitude, blood volume, vessel diameter and melanin These three tables differentiate the groups, respectively. The p-value for rejection of null hypothesis was set as 0.05.

Table 2. Test of equality of variances

Left	Levene Statistic	df1	df2	Sig.
Mie Amp	.422	2	90	.657
Mie Slope	.720	2	90	.489
Ray. Amp	2.519	2	90	.086
Blood Volume	10.461	2	90	.000
Vessel D	3.389	2	90	.038
Melanin	.528	2	90	.591
Beta Ca	2.899	2	90	.060
Saturation	1.520	2	90	.224

Table 3. Test of variances homogeneity

Middle	Levene Statistic	df1	df2	Sig.
Mie Amp	1.403	2	89	.251
Mie Slope	4.770	2	89	.011
Ray. Amp	.009	2	89	.991
Blood Volume	2.684	2	89	.074
Vessel D	.657	2	89	.521
Melanin	5.641	2	89	.005
Beta Ca	3.633	2	89	.030
Saturation	1.031	2	89	.361

Table 4. Test of variances homogeneity

Right	Levene Statistic	df1	df2	Sig.
Mie Amp	.263	2	84	.769
Mie Slope	.624	2	84	.538
Ray. Amp	3.919	2	84	.024
Blood Volume	8.264	2	84	.001
Vessel D	5.112	2	84	.008
Melanin	4.598	2	84	.013
Beta Ca	2.435	2	84	.094
Saturation	.445	2	84	.642

Table 5. Test of variances homogeneity

1st press	Levene Statistic	df1	df2	Sig.
Mie Amp	4.043	2	95	.021
Mie Slope	.790	2	95	.457
Ray. Amp	.301	2	95	.741
Blood Volume	1.451	2	95	.239
Vessel D	8.539	2	95	.000
Melanin	3.883	2	95	.024
Beta Ca	.931	2	95	.398
Saturation	2.915	2	95	.059

Table 6. Test of variances homogeneity

2nd press	Levene Statistic	df 1	df2	Sig.
Mie Amp	1.721	2	96	.184
Mie Slope	1.464	2	96	.236
Ray. Amp	2.143	2	96	.123
Blood Volume	.391	2	96	.677
Vessel D	2.147	2	96	.122
Melanin	3.453	2	96	.036
Beta Ca	.174	2	96	.841
Saturation	.054	2	96	.947

Table 7. Test of variances homogeneity

3rd press	Levene Statistic	df1	df2	Sig.
Mie Amp	.729	2	87	.485
Mie Slope	1.781	2	87	.174
Ray. Amp	2.250	2	87	.111
Blood Volume	1.250	2	87	.292
Vessel D	1.617	2	87	.204
Melanin	.004	2	87	.996
Beta Ca	1.647	2	87	.199
Saturation	1.178	2	87	.313

Among non-parametric tests, Mann-Withney test was applied for comparison of two groups and Kruskal-Wallis test was used for three groups. Tables 8-10 compare the three probe pressure levels during the measurement of the left, middle and right part of the lip, respectively. Tables 11-13 show the influence of smoking of the volunteers on the SFRS parameters for each probe pressure.

From tables 8-10 it can be concluded that the probe pressure variations could effectively change the values of the eight parameters, while Tables 11-13 show that the smoking did not have any significant influence on them.

Table 8. Test statistics [a,b]

	Mie Amp	Mie Slope	Ray. Amp	Blood Volume	Vessel D	Melanin	Beta Ca	Saturation
Chi-Square	6.280	13.351	2.615	43.682	32.503	8.200	15.514	4.120
df	2	2	2	2	2	2	2	2
Asymp. Sig.	.043	.001	.270	.000	.000	.017	.000	.127

a. Kruskal-Wallis test

b. Grouping variable: Left part

Table 9. Test statistics [a,b]

	Mie Amp	Mie Slope	Ray. Amp	Blood Volume	Vessel D	Melanin	Beta Ca	Saturation
Chi-Square	6.141	33.286	4.363	38.567	21.682	7.058	18.599	11.635
df	2	2	2	2	2	2	2	2
Asymp. Sig.	.046	.000	.113	.000	.000	.029	.000	.003

a. Kruskal-Wallis test

b. Grouping variable: Middle pressure

Table 10. Test statistics [a,b]

	Mie Amp	Mie Slope	Ray. Amp	Blood Volume	Vessel D	Melanin	Beta Ca	Saturation
Chi-Square	2.763	29.521	.933	21.019	12.988	19.186	4.372	12.978
df	2	2	2	2	2	2	2	2
Asymp. Sig.	.251	.000	.627	.000	.002	.000	.112	.002

a. Kruskal-Wallis test

b. Grouping variable: Right pressure

Table 11. Test statistics [a,b]

	Mie Amp	Mie Slope	Ray. Amp	Blood Volume	Vessel D	Melanin	Beta Ca	Saturation
Mann-Whitney U	495.000	599.000	587.500	544.000	565.000	584.000	572.000	545.000
Wilcoxon W	3981.000	719.000	707.500	4030.000	4051.000	4070.000	692.000	4031.000
Z	-1.258	-.232	-.345	-.775	-.567	-.380	-.498	-.765
Asymp. Sig. (2-tailed)	.208	.817	.730	.439	.570	.704	.618	.444

a. Grouping Variable: 1st pressure, smoking

Table 12. Test statistics [a,b]

	Mie Amp	Mie Slope	Ray. Amp	Blood Volume	Vessel D	Melanin	Beta Ca	Saturation
Mann-Whitney U	455.000	621.000	618.500	575.000	620.000	579.000	611.000	535.000
Wilcoxon W	4025.000	4191.000	4188.500	4145.000	740.000	699.000	4181.000	655.000
Z	-1.708	-.088	-.112	-.537	-.098	-.498	-.185	-.927
Asymp. Sig. (2-tailed)	.088	.930	.911	.591	.922	.619	.853	.354

a. Grouping Variable: 2nd pressure, smoking

Table 13. Test statistics [a,b]

	Mie Amp	Mie Slope	Ray. Amp	Blood Volume	Vessel D	Melanin	Beta Ca	Saturation
Mann-Whitney U	292.000	419.000	423.000	352.000	274.000	452.000	394.000	449.000
Wilcoxon W	3373.000	3500.000	501.000	430.000	352.000	530.000	472.000	3530.000
Z	-2.089	-.582	-.534	-1.377	-2.303	-.190	-.878	-.226
Asymp. Sig. (2-tailed)	.037	.561	.593	.169	.021	.849	.380	.822

a. Grouping Variable: 3rd pressure, smoking

The results obtained in this work show that the probe pressure significantly changed the descriptive parameters of SFR spectra due to three levels of probe contact pressure, while smoking was not effective on them. Independence of intrinsic fluorescence spectra to the probe pressure was shown in the human cervix [7, 9] and skin [6]. However, Ti et al. [8] showed a noticeable intensity increase in the fluorescence spectra with pressure. In contrast with fluorescence, many investigators [6, 8, 10, 11] show a meaningful dependence of reflectance to probe pressure. Our result also confirms the previous investigations while we used single fiber measurement setup.

Reif et al. [10] and Ti et al. [8] studied the probe pressure effect on the reflectance spectra in mouse. While the former group investigated the thigh muscle, the latter one tested the heart and liver of rat. Although Delgado Atencio et al. [11] and Lim et al. [6] investigated the effect on human skin, they found inconsistent results for

different parts of body [6] which confirms a site-specific difference of probe pressure effect.

In this study, the spectra acquisition time was limited to 20 – 30 ms in order to get an acceptable peak value. Accounting the delay between dark and light measurements and dummy measurements, each pressure level was applied to the tissue for less than 3 seconds. While the duration of pressure application was kept as low as reasonable in this study, most of other studies applied the pressure for several seconds [6, 10, 11] or even a few minutes [8, 9].

According to Lim et al. [6] the effects of pressure can be minimized when the pressure is small and applied for a short amount of time. In this study, the spectra acquisition time was limited to 20 – 30 ms in order to get an acceptable peak value. Accounting the delay between dark and light measurements and dummy measurements, each pressure level was applied to the tissue for less than 3 seconds. While the duration of pressure application was kept as low as reasonable in this study, most of other studies applied the pressure for several seconds [6, 10, 11] or even a few minutes [8, 9].

The magnitude of the pressure applied in this work was in agreement with the previous studies [6, 8, 10, 11]. However, the visibility of the color indicator during the spring contraction / expansion and the pain feeling of the subject during the pressure application were the most important factors to choose these levels. None of the subjects feel discomfort after the experiment.

Tables 14-16 show mean and standard deviation values of the eight parameters related to the first condition and left, middle and right parts, respectively. In these tables, it is obvious that there is an increase in the mean values for Mie amplitude, Mie slope and Rayleigh amplitude from the first pressure to second one and there is no significant variation from the second step to the third step, while considering the increase in the pressure from the first to the second level, a decrease can be seen for these values as one compares them in blood volume, vessel diameter, melanin concentration, beta carotene concentration and saturation, and again there is no noticeable changes between the values related to the second and third ones. For the second circumstance, in Tables 17-19, the mean values of the eight parameters are compared between smoking and non-smoking groups under different pressure levels. One can see that there are no different changes between the mean values of the eight parameters obtained for smoking and non-smoking groups, while it should be taken into consideration that the contribution of nonsmokers in this study is much more than volunteers who used to smoke cigarettes. A remarkable point is that increasing/decreasing trend of mean values of the parameters in smoking group is more noticeable specially by increasing the pressure from the second step to the third one.

Table 14. Mean and standard deviation values, first condition, left side

Left	N1st pres	Mean 1st	Std.	N2nd pres	Mean 2nd	Std.	N3rd pres	Mean 3rd	Std.
Mie Amp.	31	0.4814	0.0752	32	0.5288	0.08090	30	0.5200	0.0935
Mie Slope	31	-1.1034	0.3145	32	-0.8777	0.21766	30	-0.8834	0.2318
Ray. Amp.	31	0.0016	0.0070	32	0.0039	0.00698	30	0.0044	0.0076
Blood Vol.	31	0.0179	0.006	32	0.0102	0.00442	30	0.0083	0.0022
Vessel D	31	0.0262	0.0100	32	0.0180	0.00470	30	0.0161	0.0046
Melanin	31	0.1556	0.122	32	0.0980	0.08494	30	0.0979	0.0769
BetaCa	31	12.67	5.3146	32	8.7790	4.96842	30	7.6183	3.7187
Saturation	31	74.335	9.1775	32	69.9884	9.8222	30	69.7834	7.8357

Table 15. Mean and standard deviation values, first condition, middle part

Middle	N1st pres	Mean 1st	Std.	N2nd pres	Mean 2nd	Std.	N3rd pres	Mean 3rd	Std.
Mie Amp.	32	0.474	0.0891	30	0.5134	0.06891	30	0.5268	0.0643
Mie Slope	32	-1.2121	0.2812	30	-0.9342	0.18442	30	-0.8626	0.1440
Ray. Amp.	32	0.0038	0.0086	30	0.0048	0.00805	30	0.0047	0.0084
Blood Vol.	32	0.017	0.0061	30	0.0082	0.00472	30	0.0085	0.0045
Vessel D	32	0.0214	0.0061	30	0.0154	0.00564	30	0.0151	0.0051
Melanin	32	0.1669	0.1471	30	0.0970	0.08107	30	0.0844	0.0542
BetaCa	32	12.0274	5.2465	30	6.8888	3.30579	30	7.9368	3.8394
Saturation	32	76.6405	8.5726	30	70.2422	7.21206	30	69.4676	9.4697

Table 16. Mean and standard deviation values, first condition, right side

Right	N1st pres	Mean 1st	Std.	N2nd pres	Mean 2nd	Std.	N3rd pres	Mean 3rd	Std.
Mie Amp.	30	0.4917	0.0649	31	0.4992	0.0669	31	0.5244	0.0696
Mie Slope	30	-1.0595	0.215	31	-0.8550	0.1563	31	-0.7667	0.1677
Ray. Amp.	30	0.0006	0.0023	31	0.0021	0.0056	31	0.0016	0.0034
Blood Vol.	30	0.0191	0.0081	31	0.0123	0.0044	31	0.0110	0.0044
Vessel D	30	0.028	0.0157	31	0.0197	0.0047	31	0.0195	0.0048
Melanin	30	0.1898	0.0977	31	0.1069	0.0619	31	0.0873	0.0577
BetaCa	30	11.952	7.3587	31	9.8481	5.6503	31	8.2584	3.7540
Saturation	30	74.9923	8.8846	31	67.6126	8.3595	31	67.4162	7.6140

Table 17. Mean and standard deviation values, second condition, 1st Pressure

1st Pressure	N Non Smoking	Mean Non Smoking	Std. Non Smoking	N Smoking	Mean Smoking	Std. Smoking
Mie Amp.	83	0.4801	0.0791	15	0.5074	0.04718
Mie Slope	83	-1.1054	0.2760	15	-1.1747	0.36133
Ray. Amp.	83	0.0018	0.0065	15	0.0024	0.00679
Blood Vol.	83	0.0183	0.007	15	0.0203	0.00876
Vessel D	83	0.0261	0.01236	15	0.0318	0.02015
Melanin	83	0.1752	0.1194	15	0.2015	0.17138
BetaCa	83	13.1278	7.1325	15	11.4885	4.82725
Saturation	83	74.397	9.0697	15	78.0881	13.3254

Table 18. Mean and standard deviation values, second condition, 2nd Pressure

2nd Pressure	N Non Smoking	Mean Non Smoking	Std. Non Smoking	N Smoking	Mean Smoking	Std. Smoking
Mie Amp.	84	0.5089	0.07266	15	0.5388	0.06110
Mie Slope	84	-0.8884	0.1965	15	-0.9069	0.25711
Ray. Amp.	84	0.0034	0.0068	15	0.0061	0.01185
Blood Vol.	84	0.0102	0.0048	15	0.0104	0.00386
Vessel D	84	0.0179	0.0059	15	0.0170	0.00362
Melanin	84	0.1042	0.0769	15	0.1215	0.16559
BetaCa	84	8.9341	5.1654	15	9.4589	6.01679
Saturation	84	68.9782	9.1567	15	67.1057	10.02863

Table 19. Mean and standard deviation values, second condition, 3rd Pressure

3rd Pressure	N Non Smoking	Mean Non Smoking	Std. Non Smoking	N Smoking	Mean Smoking	Std. Smoking
Mie Amp.	78	0.5161	0.0763	12	0.5679	0.06466
Mie Slope	78	-0.8409	0.1928	12	-0.8237	0.16115
Ray. Amp.	78	0.0038	0.0072	12	0.0013	0.00325
Blood Vol.	78	0.0095	0.0043	12	0.0077	0.00223
Vessel D	78	0.0176	0.0061	12	0.0140	0.00294
Melanin	78	0.0926	0.0672	12	0.0864	0.06150
BetaCa	78	8.4387	4.0806	12	7.4720	4.12161
Saturation	78	67.968	9.6283	12	69.4635	6.67906

Chapter 5

CONCLUSION

Present study investigated the effect of probe pressure via in vivo measurement of reflectance spectra from left, middle and right part of the lower lip of the subjects. The spectra were obtained by the single fiber reflectance spectroscopy method. We determined whether the pressure variation would affect the reflectance spectra from each measured point and if smoking would generally influence the obtained spectra. Kruskal-Wallis and Mann-Whitney tests were used for finding a significant difference between the groups under investigation. The results showed that smoking does not affect the extracted parameters, while pressure changes all eight parameters. These are summary of the thesis not a conclusion. Conclusion means for example advising the smokers to continue their behavior or the researchers to consider the probe pressure during SFR measurements. Or, maybe declaring that the sample size was not enough to conclude something!

REFERENCES

[1] Steve Jaques, Phys. Med. Biol. 58 (2013) R37–R61,

[2], Welch A J and van Gemert M J C 2011 Overview of optical and thermal laser-tissue interaction and nomenclature Optical-Thermal Response of Laser-Irradiated Tissue 2nd edned A J Welch and M J C van Gemert (Berlin: Springer) chapter 1 (DOI:10.1007/978-90-481-8831-4)

[3] Prahl S A and Jacques S L 2012 http://omlc.ogi.edu/software/mie/ Mie theory

[4] S. Kanick, U. Gamm, M. Schouten, H. Sterenborg, D. Robinson, and A. Amelink, "Measurement of the reduced scattering coefficient of turbid media using single fiber reflectance spectroscopy: fiber diameter and phase function dependence," Biomed Opt Express, vol. 2, pp. 1687-1702, 2011.

[5] Arjen Amelink, Henricus J. C. M. Sterenborg, Martin P. L. Bard, and Sjaak A. Burgers: In vivo measurement of the local optical properties of tissue by use of differential path-length spectroscopy; Optics Letters, Vol. 29, Issue 10, pp. 1087-1089 (2004) http://dx.doi.org/10.1364/OL.29.001087

[6] L. Lim, B. Nichols, N. Rajaram, and J. Tunnell, "Probe pressure effects on human skin diffuse reflectance and fluorescence spectroscopy measurements," J Biomed Opt, vol. 16, p. 011012, 2011.

[7] K. Rivoire, A. Nath, D. Cox, E. N. Atkinson, R. Richards-Kortum, and M. Follen, "The effects of repeated spectroscopic pressure measurements on fluorescence intensity in the cervix," Am J ObstetGynecol, vol. 191, pp. 1606-1617, 2004.

[8] Y. Ti and W.-C. Lin, "Effects of probe contact pressure on in vivo optical spectroscopy," Opt. Exp., vol. 16, pp. 4250-4262, 2008.

[9] A. Nath, K. Rivoire, S. Chang, D. Cox, E. Atkinson, M. Follen, and R. Richards-Kortum, "Effect of probe pressure on cervical fluorescence spectroscopy measurements," J Biomed Opt, vol. 9, pp. 523-533, 2004.

[10] R. Reif, M. Amorosino, K. Calabro, O. A'Amar, S. Singh, and I. Bigio, "Analysis of changes in reflectance measurements on biological tissues subjected to different probe pressures," J Biomed Opt, vol. 13, p. 010502, 2008.

[11] J. A. D. Atencio, E. E. O. Guillén, S. V. y. Montiel, M. C. Rodríguez, J. C. Ramos, J. L. Gutiérrez, and F. Martínez, "Influence of Probe Pressure on Human Skin Diffuse Reflectance Spectroscopy Measurements," OPTICAL MEMORY AND NEURAL NETWORKS (INFORMATION OPTICS), vol. 18, pp. 6-14, 2009.

[12] A.N. Mustapa, Z.A. Manan , C.Y. MohdAzizi , W.B. Setianto, A.K. Mohd Omar, (2011) Extraction of b-carotenes from palm oil mesocarp using sub-critical R134a

[13] Sanaz Hariri Tabrizi, S Mahmoud Reza Aghamiri, Farah Farzaneh,ArjenAmelink, Henricus J C M Sterenborg Single fiber reflectance

spectroscopy on cervical premalignancies: the potential for reduction of the number of unnecessary biopsies.

[14] George Zonios, Julie Bykowski, and NikiforosKollias Skin Melanin, Hemoglobin, and Light Scattering Propertiescan be Quantitatively Assessed In Vivo Using Diffuse Reflectance Spectroscopy; J Invest Dermatol 117:1452±1457, 2001

[15] Steven Jacques, http://omlc.ogi.edu/spectra/melanin/index.html

[16] S. C. Kanick, D. J. Robinson, H. J. C. M. Sterenborg, and A. Amelink, "Monte Carlo analysis of single fiber reflectance spectroscopy: photon path length and sampling depth," Physics in Medicine and Biology, vol. 54, pp. 6991-7008, 2009.

[17] S. C. Kanick, D. J. Robinson, H. J. C. M. Sterenborg, and A. Amelink, "Method to quantitate absorption coefficients from single fiber reflectance spectra without knowledge of the scattering properties," Opt Lett, vol. 36, pp. 2791-2793, 2011.

[18] A. Amelink, D. Robinson, and H. J. C. M. Sterenborg, "Confidence intervals on fit parameters derived from optical reflectance spectroscopy measurements," J. Biomed.Opt., vol. 13, p. 054044, 2008.

[19] A. Amelink, T. Christiaanse, and H. J. C. M. Sterenborg, "Effect of hemoglobin extinction spectra on optical spectroscopic measurements of blood oxygen saturation," Opt Lett, vol. 34, pp. 1525-1527, 2009.

[20] S. W. v. d. Poll, "Raman spectroscopy of atherosclerosis," in ISBN 90-9016109-0. vol. PhD Leiden: University of Leiden, 2003, p. 123.

[21] S. C. Kanick, C. v. d. Leest, J. G. J. V. Aerts, H. C. Hoogsteden, S. Kaščáková, H. J. C. M. Sterenborg, and A. Amelink, "Integration of single-fiber reflectance spectroscopy into ultrasound-guided endoscopic lung cancer staging of mediastinal lymph nodes," Journal of Biomedical Optics, vol. 15, p. 017004, 2010.